High-power, ultrasonic fatigue testing machine

J. K. Tien, S. Purushothaman, R. M. Arons, J. P. Wallace, O. Buck, H. L. Marcus, R. V. Inman, and G. J. Crandall

Citation: Review of Scientific Instruments **46**, 840 (1975); doi: 10.1063/1.1134350
View online: http://dx.doi.org/10.1063/1.1134350
View Table of Contents: http://scitation.aip.org/content/aip/journal/rsi/46/7?ver=pdfcov
Published by the AIP Publishing

High-power, ultrasonic fatigue testing machine

J. K. Tien, S. Purushothaman, R. M. Arons, and J. P. Wallace

Henry Krumb School of Mines, Columbia University, New York, New York 10027

O. Buck, H. L. Marcus, R. V. Inman, and G. J. Crandall

Science Center, Rockwell International, Thousand Oaks, California 91360

(Received 9 December 1974; in final form, 14 March 1975)

A machine capable of fatigue testing high strength alloys at an ultrasonic frequency (20 kHz), and a range of temperatures likely to be encountered by such materials in aerospace and power generation applications and in basic research, is described. The machine is assembled entirely from commercially available components used in ultrasonic joining processes. Basically, it consists of a power supply module and heavy duty transducer capable of delivering up to 1.2 kW of acoustic energy at peak-to-peak amplitudes ranging from 10 to 20 μ, which is further amplified by tuned acoustic horns. The machine sets up a 20 kHz standing wave in the resonant test specimen. Peak-to-peak displacement amplitudes in the specimen of up to 300 μ (typical stress levels up to 1400 MN/m^2) can be achieved. Provisions have also been made to accurately monitor the frequency of testing and the displacement amplitude during the test. As an example of the capabilities of the machine, results of high-frequency fatigue tests performed over a range of temperatures are presented. Lastly, it is indicated that ultrasonic fatigue testing, by virtue of its extremely high rate of testing, can be conveniently used for the study of very slow fatigue crack propagation in engineering alloys.

INTRODUCTION

Dynamic resonant fatigue loading and attendant failure of the components of high speed machinery used in aerospace and power generation applications have made it necessary to evaluate and understand the mechanical behavior of materials at extremely high deformation rates. Failure of gas turbine blades in resonant fatigue is a typical example of this kind of dynamic failure. Conventional fatigue testing machines are not capable of simulating this extremely high-frequency (of the order of 20 kHz) loading, and due to the strong influence of strain rate on the mechanical behavior of materials, the available data determined at conventional frequencies cannot be recommended for design purposes at high frequencies with any good reliability. Hence, the need for a testing system that can carry out fatigue tests of the strong engineering alloys at high frequencies of the order of 20 kHz seems imperative. Such a system should be capable of generating, controlling, and measuring stress or strain levels high enough to cause fatigue damage in these alloys, and should allow testing at the elevated temperatures which the specimens experience during their service life. Such a machine, operating at high frequencies, will reduce the testing time by at least three orders of magnitude over conventional testing machines, and hence will be an extremely rapid and handy fatigue testing device, as will be shown later in this article.

In this article one such testing system, assembled entirely from commercially available components used in ultrasonic joining processes, is described. This machine has been used successfully for many years.[1] Typical results of ultrasonic fatigue tests on a gas turbine blade alloy, Mar-M-200,[2] will be presented. Lastly, a potential application of ultrasonic fatigue testing to threshold fatigue crack propagation and problems related to this application will be discussed.

DESIGN PRINCIPLES AND APPARATUS DESCRIPTION

When a solid rod of length L is subjected to an acoustic wave of wavelength $2L$ at one end, a standing wave is set up in the rod due to the interaction of the main wave and the wave reflected from the other end. In the usual wave notation, the displacement variation along the length of such a resonant rod subjected to a longitudinal acoustic wave is given by

$$U(x,t) = U_m \cos(\pi x/L) \sin(\omega t), \tag{1}$$

where $U(x,t)$ is the displacement at a distance x from one end of the rod at time t; U_m is the maximum value of $U(x,t)$, which occurs at either end of the rod; $\omega = (2\pi/\lambda)\sqrt{E/\rho}$ is the frequency of the exciting wave, where λ is the wavelength of the acoustic wave (which equals twice the length of the rod); L is the length of the rod; and E and ρ are the Young's modulus and the density of the rod, respectively. Differentiating Eq. (1) with respect to x, the strain distribution is obtained as

$$\epsilon(x,t) = \partial U(x,t)/\partial x = -(\pi/L) U_m \sin(\pi x/L) \sin(\omega t). \tag{2}$$

These displacement and strain variations along the length of the rod are shown in Fig. 1. The corresponding stress

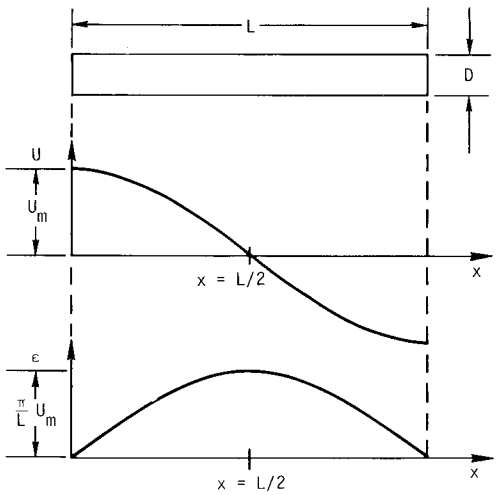

FIG. 1. Variations of maximum displacement (center) and corresponding strain (bottom) along the length of a test rod (top) subjected to an acoustic wave of the appropriate resonant frequency.

distribution is given by

$$\sigma(x,t) = E\epsilon(x,t). \tag{3}$$

It is clear that one can achieve cyclic straining of the resonant rod at any desired high frequency by properly choosing the length of the rod. The only difference between conventional fatigue testing and such high-frequency resonant fatigue testing (other than the higher frequency involved) is the fact that in the latter, cyclic strain amplitude varies from zero at the ends to a maximum at the center of the test specimen, rather than being constant over the entire length. This has the advantage of confining fatigue damage and, hence, crack initiation to the center of the specimen.

The acoustic excitation of the test rod is achieved by an arrangement which is very similar to the one used for measurement of internal friction in solids at high

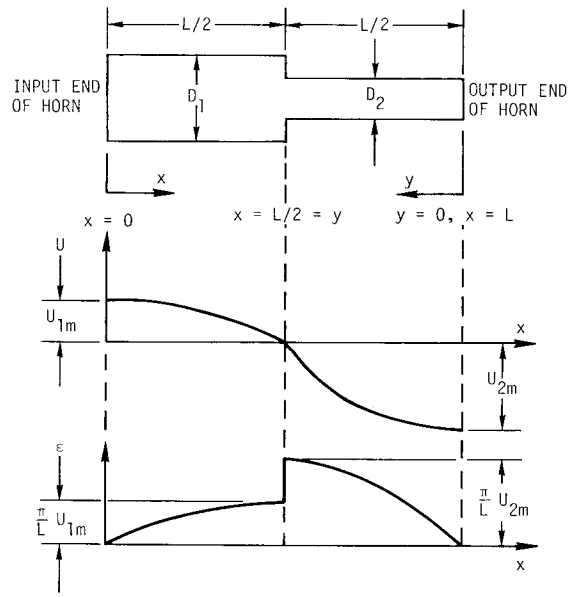

FIG. 2. Variations of maximum displacement (center) and corresponding strain (bottom) along the length of a "step horn" (top) under resonant conditions.

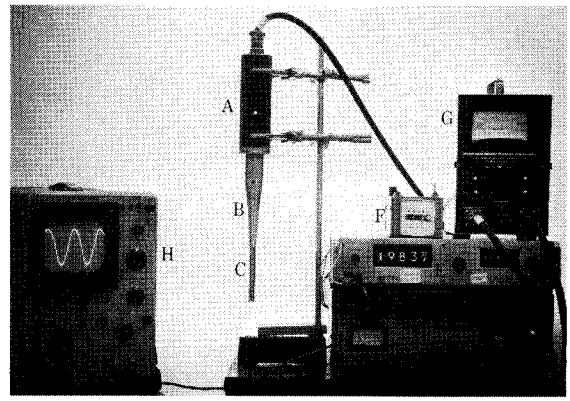

FIG. 3. Typical ultrasonic fatigue test assembly and accompanying instrumentation. A—Transducer housing; B—horn; C—test specimen; D—power supply module; E—frequency counter; F—timer; G—wattmeter; H—oscilloscope.

frequencies,[3] but is capable of much higher displacement and power levels. Excitation is achieved by a heavy-duty lead zirconium titanate (PZT) transducer manufactured by Branson Sonic Power Co., which is capable of delivering displacement amplitudes in the range of 10–20 μ at 20 kHz when used with an appropriate power supply manufactured by the same company. This acoustic amplitude is further stepped up by the use of acoustic amplifier horns. The design of these horns was pioneered by Mason[3] and Neppiras.[4] The horns are rods of resonant length whose cross-sectional area decreases either continuously or discontinuously with distance from the input (driving transducer) end. In order to meet the physical requirement of continuity of particle velocity along the length of the horn, the vibrational amplitude has to increase in regions of reduced area, thus achieving displacement and strain amplification.

Consider, for example, the case of a step horn which, as shown in Fig. 2, has a section of length $L/2$ with a larger cross section ($A_1 = \pi/4D_1^2$) connected to a smaller cross section ($A_2 = \pi/4D_2^2$) of equal length $L/2$, L being the half wavelength at the frequency of interest. In the large diameter sections, the displacement and strain along the lengths are given by the equations

$$\begin{aligned} U_1(x,t) &= U_{1m}\cos(\pi x/L)\sin(\omega t) \\ \epsilon_1(x,t) &= -(\pi/L)U_{1m}\sin(\pi x/L)\sin(\omega t), \end{aligned} \tag{4}$$

where x is measured from the input end of the horn, as shown in Fig. 2. In the small diameter section, the displacement and strain are given by

$$\begin{aligned} U_2(y,t) &= U_{2m}\cos(\pi y/L)\sin(\omega t) \\ \epsilon_2(y,t) &= -(\pi/L)U_{2m}\sin(\pi y/L)\sin(\omega t), \end{aligned} \tag{5}$$

where y is the distance measured from the output end of the horn, again as shown in Fig. 2. Continuity of displacement is automatically satisfied at the point of sudden change of the cross section. In order to balance the total force transmitted at the point of area change, one has to invoke, assuming an elastic standing wave,

$$A_1E\epsilon_1(x=L/2,\,t) = A_2E\epsilon_2(y=L/2,\,t). \tag{6}$$

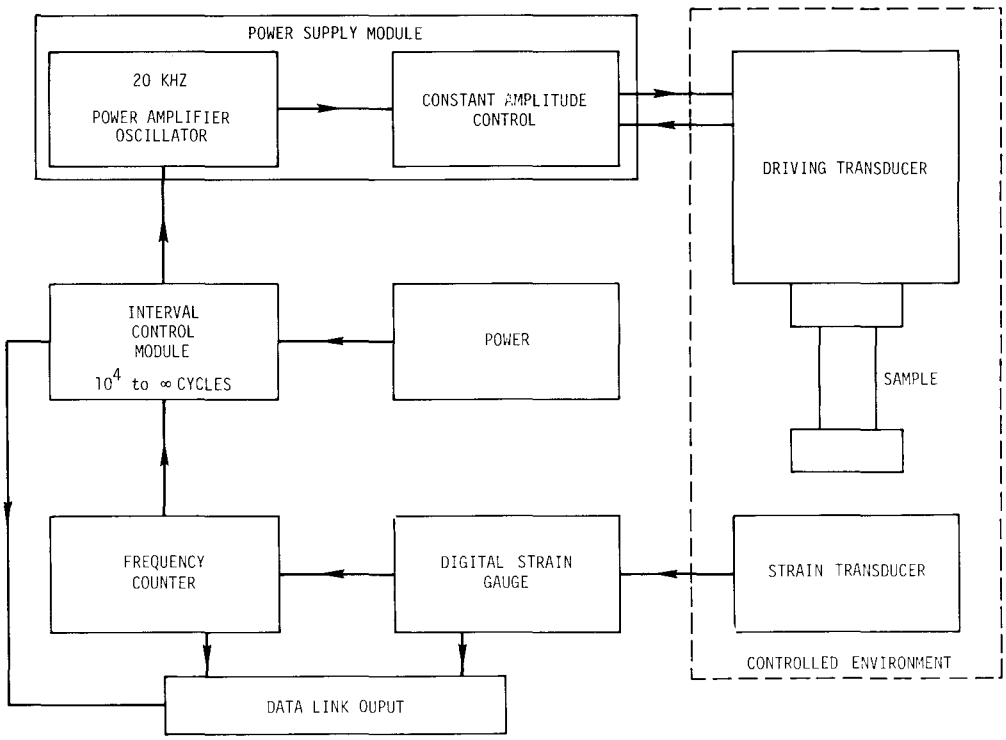

FIG. 4. Ultrasonic fatigue unit (schematically).

This implies that

$$-(\pi/L)U_{1m}A_1E=-(\pi/L)U_{2m}A_2E$$

or

$$U_{2m}/U_{1m}=A_1/A_2, \tag{7}$$

which means that the displacement and, hence, strains are amplified by the ratio of the cross-sectional areas for the horn. Similar derivations can be made for horns of other shapes, such as one with an exponential taper from input to output. Also, by suitably designing the shape of the specimen, one can achieve strain amplification in a selected region of the specimen. Calculations of this kind have been done by Mason[3] and Neppiras.[4]

Thus, by the use of a selected train of horns or proper specimen design, one can achieve any desired cyclic strain amplitude in the resonant rod connected to the horn. A typical assembly for ultrasonic fatigue testing is shown in Fig. 3. All connections at the acoustic junctions (such as transducer to horn or horn to test rod) are done by the use of set screws. There is no problem of screw failure, since these junctions are nodal points of strain and hence are stress free.

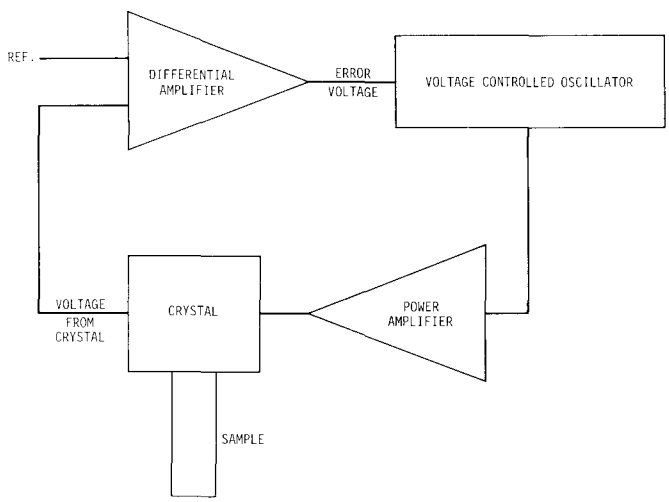

FIG. 5. Feedback loop for constant amplitude in ultrasonic fatigue.

An illustrative schematic of the testing system is shown in Fig. 4. A variable exciting voltage is supplied to the driving transducer by the power supply module, which houses a 20 kHz power amplifier capable of delivering up to 1.2 kW of energy and a constant amplitude control that maintains the amplitude of vibration of the system well within 10% of the set value, even if the resonant frequency of the sample changes. This power supply module and the heavy duty transducer, both commercially deployed in ultrasonic joining processes, are the main features of this test system that have enabled the testing of very strong materials at high cyclic strain amplitudes. The system demands high power capabilities, nearly 100 W, when the test rod is in resonance at a strain amplitude of nearly 5×10^{-3}, increasing to higher wattage when the test rod fails in ultrasonic fatigue. Such fatigue testing capabilities could not be achieved in the earlier systems of similar nature designed and used for internal friction

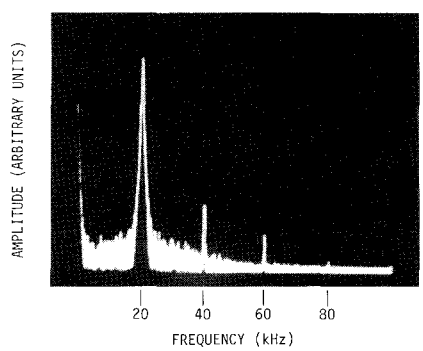

FIG. 6. Spectrum analysis of the displacement at the free end of a cracked specimen.

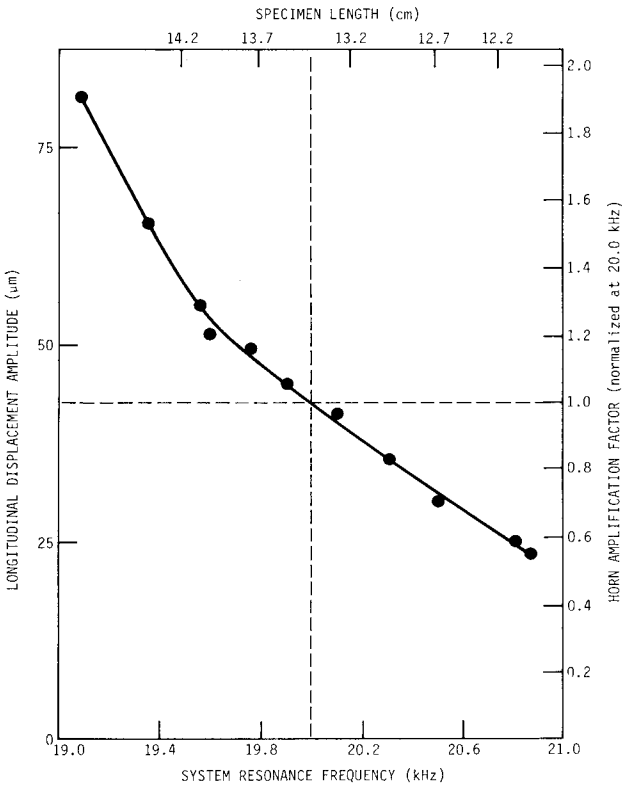

FIG. 7. Variation of longitudinal displacement amplitude with system resonance frequency.

measurements by Mason[3] and, subsequently, by his coworkers,[5] and independently by Neppiras.[4] The interval control module is essentially a timer which can turn the power supply on for any preset length of time and record the number of cycles elapsed since the start. The item marked "sample" represents the train of horns and the sample in the actual system. The combination of the driving train, the sample, and the strain transducer can be enclosed in a chamber of controlled environment for simulation of actual service conditions. Figure 5 shows the details of the constant-amplitude control circuit. A pickup voltage from the crystal transducer is compared in a differential amplifier with a reference voltage set according to the amplitude desired. The differential amplifier puts out an amplifier error voltage which corrects the voltage-controlled oscillator. The corrected output of the voltage-controlled oscillator is amplified by the power amplifier and fed into the crystal transducer. In this way the displacement amplitudes are kept within 10% of any desired level, even if the resonant frequency of the sample drifts due to structural damage under cycling, cracking, or temperature rise resulting from the internal friction of the sample.

The strain and frequency are measured directly, as shown in the schematic, and the information can be stored in magnetic tape devices which can interface with the data-link output. Typical measuring devices for such high-frequency displacement monitoring are based on fiber optics, eddy current, or capacitance detection techniques, and employ noncontact measuring probes. A capacitance displacement gauge capable of $\pm 0.1\%$ accuracy and nearly $3\times10^{-2}\,\mu$ sensitivity, manufactured by ADE Corp., was found to be well suited for displacement monitoring. Selection of an instrument with sufficient frequency response even allowed monitoring of higher harmonics of the fundamental fatigue frequency. Such a spectrum analysis of the longitudinal displacement at the free end of a cracked specimen is shown in Fig. 6.

A typical plot of displacement amplitude U_m at the end of an aluminum sample at various values of sample resonant frequency is shown in Fig. 7. These data were obtained by exciting Al alloy rods of various resonant frequencies (various lengths), with the resonant fatigue apparatus and measuring the amplitude of vibration at the free end. In the normal range of operating frequency, between 19.5 and 20.5 kHz, the vibrational amplitude is seen to be within 30% of the value at 20 kHz. Except near the very end of the test period, when large-scale fatigue cracking of the test rod occurs, the resonant frequency changes are never more than ± 50–100 Hz from the starting frequency, provided the test rod is cooled by a stream of air and the amplitude changes are well within 5%–10%.

Elevated temperature testing can be carried out simply by surrounding the sample by a small resistance furnace and heating it to the required temperature. Use of induction heating is also being contemplated. A typical setup for elevated temperature work is shown in Fig. 8. Here, it is necessary to introduce a series of 1:1 acoustic transformers in the assembly to provide enough separation between the transducer and the hot test rod, since overheating of the transducer can damage it and affect its

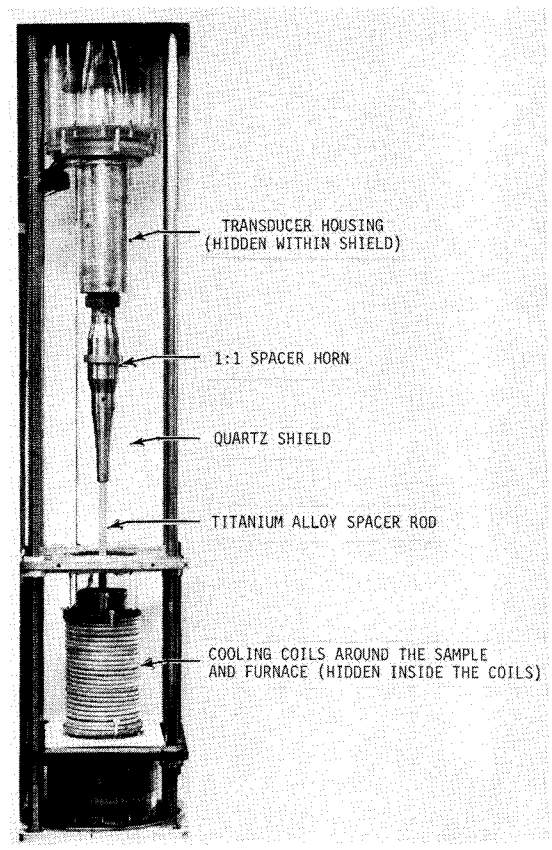

FIG. 8. Ultrasonic fatigue test assembly for high-temperature testing.

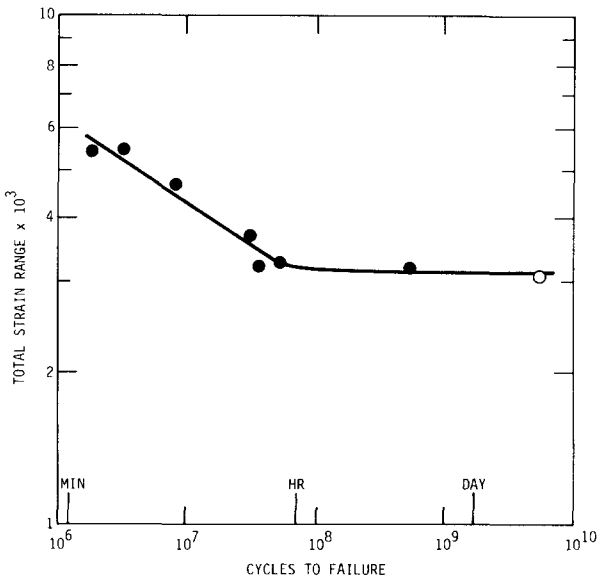

FIG. 9. Ultrasonic fatigue behavior of Mar-M-200 single crystals showing number of cycles to failure at different total strain range values (300 K). ●—Failure; ○—no failure.

efficiency. Test temperatures up to about 1200 K have been successfully employed without much difficulty.

Having discussed the major characteristics of the ultrasonic fatigue testing machine, one should also mention some points of caution regarding its applications. Firstly, the rise time (or decay time) of the amplitude when the machine is turned on (or off) is of the order of 0.5 sec. Therefore, tests lasting less than this amount of time (less than 10^4 cycles) cannot be conducted with this machine. Secondly, due to the extremely rapid rate of strain cycling involved in these tests, the temperature of the test specimen would rise very rapidly to a high steady-state value as a result of internal friction losses in the test material. However, it was found that in systems of low internal friction, such as the nickel-base alloys, this temperature rise is not more than 10°C. In alloys with intermediate internal friction, such as the Al alloys, the temperature rise can be kept reasonably small by cooling the test specimen by a stream of air. Hence, it is thought that internal friction heating would not be a major stumbling block in the testing of most engineering alloys which possess low or intermediate internal friction characteristics. However, water or some other liquid may have to be used for cooling materials of very high internal friction, such as iron-base alloys or steels. This may result in some complications, since the interaction of the coolant with the test material could change the fatigue characteristics of the material itself through, for example, premature crack initiation of the surface. In these cases, caution should be exercised to note the effects of such interactions in interpreting the test results, and to this extent the applications of ultrasonic fatigue testing to high internal friction materials is of restricted value only.

Lastly, one could question the validity of ultrasonic fatigue testing on the basis that the strain is not uniform over the entire length of the test bar. As mentioned earlier, this acts only to confine crack initiations to the center of the test bar. However, if one prefers, it is possible to achieve a reasonably constant and high strain along a certain length at the central part of the specimen while maintaining a low value of strain at either end of the specimen. This can be achieved by simply choosing a dumbbell-shaped resonant specimen geometry, where the flanges of the dumbbell are of larger diameter and, hence, carry a lower strain compared to the central part of the dumbbell. Mason[3] has used this geometry for achieving high constant strains in his specimens employed in internal friction measurements. Similar suggestions have also been made by Neppiras[4] in his studies.

In summary, one can say that the ultrasonic fatigue testing assembly fulfills all the basic needs enumerated in the Introduction: it provides a means for cyclically stressing materials, especially materials with low internal friction, over a wide range of temperatures at a high frequency and at high strain amplitudes, which can be controlled and accurately measured.

Having shown that the system fulfills the requirements for high-frequency fatigue testing, results of some of the tests done using the system on Ni-base superalloy Mar-M-200 are presented and discussed in the next section.

RESULTS OF ULTRASONIC FATIGUE TESTS OF SUPERALLOY MAR-M-200

Figure 9 shows a typical S–N curve generated at 20 kHz for single crystals of Mar-M-200, a typical superalloy used in present-day gas turbine blades.[6] It should be mentioned that this is the first time that a well-defined fatigue limit has been found for this alloy. This was made possible because the fatigue test at 20 kHz could be run for 10^{10} cycles within a period of a week, owing to the rapid testing rate. Conventional fatigue testing at 10 Hz would have taken nearly 35 years for the same number of cycles. So, apart from being an invaluable technique to simulate extremely high-frequency dynamic loading conditions, ultrasonic fatigue testing also turns out to be an extremely rapid technique for evaluating materials. Thus, if one can normalize the fatigue deformation behavior of materials with respect to deformation rates, then one can conduct the fatigue tests at ultrasonic frequency within

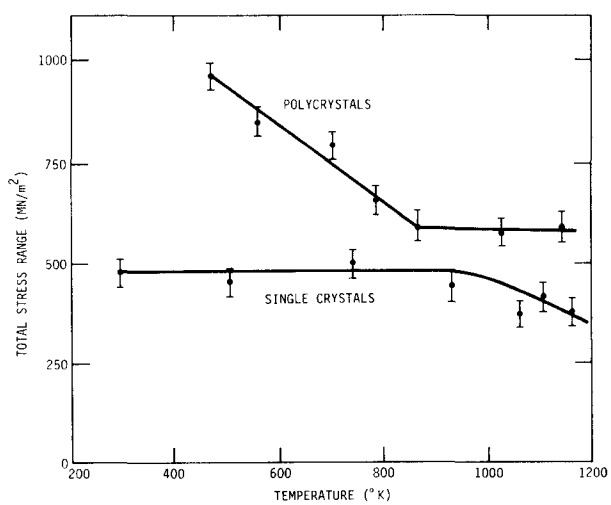

FIG. 10. 5×10^6 cycle endurance limit of Mar-M-200 single crystals and polycrystals as a function of temperature at 20 kHz.

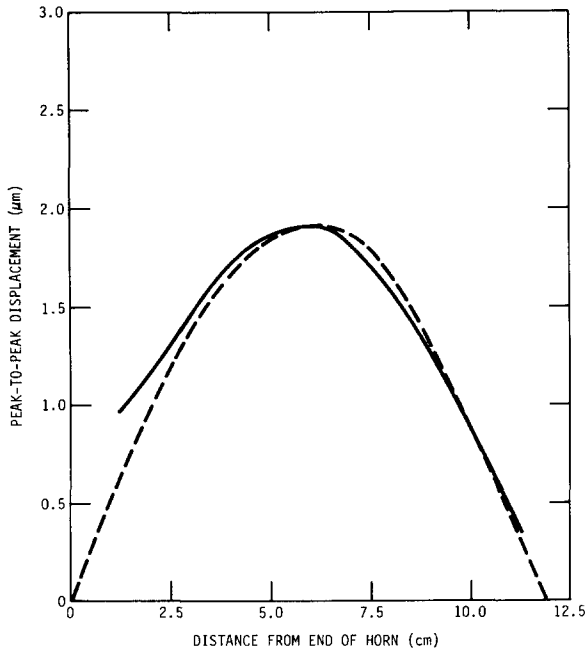

FIG. 11. Radial peak-to-peak displacement along the length of a 1.9-cm-diam smooth specimen (no slit). Al 6061-T6; $f_0=20.045$ kHz; $U_m=22.5\ \mu$. ——Average of four measurements; - - - -Poisson [Eq. (8)].

an extremely short length of time and extrapolate to the fatigue behavior at low frequency when necessary. In fact, the knowledge of strain rate dependence of deformation behavior in Mar-M-200 single crystals has been used to compare low-frequency and ultrasonic-frequency fatigue test data. An interesting and important interaction between the test environment and the fracture and crack propagation process in this superalloy has thereby been identified.[6]

In Fig. 10, the temperature dependence of the 5×10^6 cycle endurance limit at 20 kHz for single-crystal and polycrystalline Mar-M-200 is shown. This is, again, the first set of data obtained on the dynamic resonant loading of this superalloy over a wide range of temperature.[6]

APPLICATION OF ULTRASONIC FATIGUE TO THRESHOLD CRACK PROPAGATION STUDIES

It is widely believed that, in many metals and alloys, most of the fatigue life is spent in initiating a propagatable microcrack and in the initial stages of its growth (when the stress intensity factor, i.e., the applied stress amplification due to the stress concentration at the crack tip, is low). In this early crack growth period, also known as the threshold period, the crack growth rate per cycle of stress is very small owing to the small value of the driving force for crack growth, namely, the stress intensity. So, in order to obtain a physically measurable change in the crack length, one has to cycle the material over a large number of cycles, which means a very long period of time at conventional test frequencies. Therefore, high-frequency fatigue testing could provide a means of conveniently and quickly measuring threshold crack growth rates in materials, which can lead to a better understanding of the mechanisms underlying fatigue failure.

However, it should be recognized that in an ultrasonic fatigue crack propagation test, the test rod has a single propagating fatigue crack during the entire duration of the test, and hence it is imperative to know how, if at all, this would affect the longitudinal resonance conditions in the rod. This knowledge is also pertinent to the case of materials in which crack propagation occupies a considerable part of their fatigue life.

Since the introduction of a crack in the test rod causes asymmetry in the transfer of forces across the crack plane, a flexural mode of vibration of the test rod could be excited, provided there exists a flexural mode whose frequency is at the driving frequency. If this occurs, the stress state at the tip of the crack would be modified due to the flexural stresses superposed on the longitudinal stresses.

To verify whether such a modification indeed occurs, one has to measure the lateral displacement amplitude of the sample. In the ideal case of a pure longitudinal resonance one would expect to see the Poisson contraction as a result of the longitudinal strain, and the measured amplitude would be

$$V=\nu(\pi/L)U_m(D/2)\sin(\pi x/L), \tag{8}$$

where V is the lateral displacement amplitude, ν is the Poisson ratio of the rod material, and D is the diameter of the rod (U_m and L were defined earlier).

However, if a flexural mode is being excited by the crack, then the amplitude measured on the side will be a superposition of the lateral displacement and the flexural contribution. Therefore, by comparing the measured amplitude and the material displacement one can determine the flexural amplitude variation and identify the particular flexural mode. Additional contribution of stresses due to this flexure at the crack plane can be computed and compared with the magnitude of the longitudinal stresses.

The above-mentioned studies were conducted in the

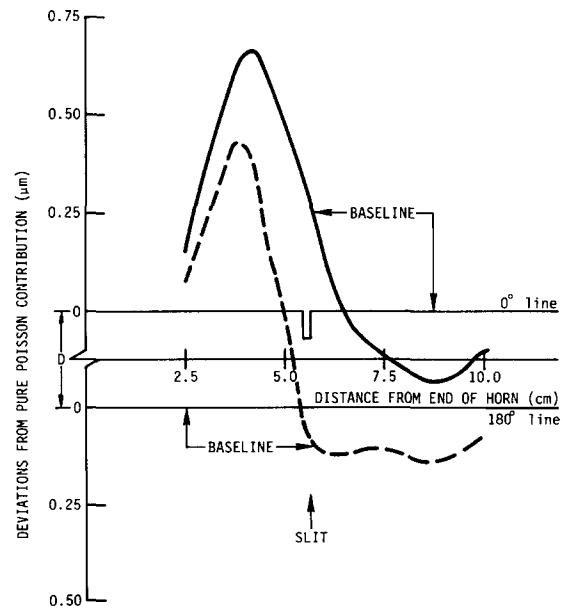

FIG. 12. Deviation of the lateral displacement from the Poisson contribution due to a 3 mm slit. Al 6061-T6; $f_0=19.997$ kHz; $U_m=22.8\ \mu$. ——0° line (over crack); - - - -180° line (behind crack).

following manner. The validity of Eq. (8) was verified by measuring the lateral amplitudes along the length of a 1.9-cm-diam smooth Al alloy specimen, along four lines 90° apart from each other (labeled 0°, 90°, 180°, and 270°, respectively). It was found that all four profiles were nearly identical and conformed to the value expected from Eq. (8), as shown in Fig. 11.

Then, a thin artificial crack was introduced in depth increments of 1 mm at the center of the specimen at the 0° line by electrospark cutting and the lateral amplitudes were again measured. The amplitudes measured at the 90° and 270° lines were hardly different from their form before slitting, while the 0° and 180° amplitudes showed deviations from the expected Poisson contribution. These deviations are shown in Fig. 12 as displacement amplitudes on the surface of the rod. They represent very closely a flexural mode which is set up by the presence of the crack and which, in a first approximation, may be given as the second harmonic of a free–free flexural vibration whose frequency f is given by[7]

$$f=(30.836/\pi L^2)R(E/\rho)^{\frac{1}{2}}. \quad (9)$$

This vibration is forced by the longitudinal vibration and therefore $f=19.997$ kHz. Using appropriate values for the radius of gyration R, E, and ρ the length L necessary to fulfill Eq. (9) is very close to the actual specimen length.

Similar deviations from a Poisson contribution were found in test rods of 1.5 cm. Applying the same type of analysis as before, the third harmonic of a free–free flexural vibration, forced by the longitudinal vibration, was obtained.

Next, the contribution of these flexural vibrations to the stresses in the crack plane were calculated. Analytical forms of the amplitude variation along the length in these flexural modes were used[7] and from simple isotropic elastic beam bending type analysis,[8] peak surface stresses were found not to exceed 7×10^5 N/m^2 ($\sim$100 psi). Since the lowest values of longitudinal stresses that may be employed in crack propagation studies and fatigue tests of the high-strength engineering alloys are of the order of 10^8 N/m ($\sim$15 000 psi), the stress contribution due to flexural vibrations is insignificant. Hence, one can confidently state that the complications due to flexural stresses in resonant fatigue test specimens can be ignored and ultrasonic fatigue testing can be used for the study of threshold crack propagation without trepidation.

ACKNOWLEDGMENT

We are extremely grateful to Dr. W. L. Morris for his diligent review of this paper and for his suggestions on the physics of flexural vibrations.

[1]J. K. Tien and R. P. Gamble, Met. Trans. **2**, 1933 (1971).
[2]Mar-M-200: 9 Cr, 10 Co, 2 Ti, 5 Al, 12.5 W, 1 Nb, 0.015 B, 0.06 Zr, and balance Ni. (all wt. %).
[3]W. P. Mason, in *Microplasticity*, edited by C. J. McMahon (Wiley, New York, 1968).
[4]E. A. Neppiras, Proc. ASTM **59**, 691 (1959).
[5]D. E. MacDonald and W. A. Wood, J. Appl. Phys. **42**, 5531 (1971).
[6]S. Purushothaman, J. P. Wallace, and J. K. Tien, in *Proceedings of Ultrasonic International* (IPC, London, 1973), p. 244.
[7]A. S. Nowick and B. S. Berry, *Anelastic Relaxations in Crystalline Solids* (Academic, New York, 1972), pp. 626–629.
[8]P. G. Laurson and W. J. Cox, *Mechanics of Materials* (Wiley, New York, 1974), pp. 152–158.